

Construction of a feedback control system based on CFD simulations for the 64-element Canadian SCWR

Huirui Han, Chao Zhang*

Department of Mechanical & Materials Engineering, Western University, 1151 Richmond Street, London, ON, N6A 5B9, Canada



ARTICLE INFO

Keywords:

Computational fluid dynamics
Linear dynamic model
Controller
Feedback control

ABSTRACT

The knowledge of the dynamic behaviors of the supercritical water in the fuel bundle of the nuclear reactor is necessary for the design of the control system. For this purpose, the transient full-scale computational fluid dynamics (CFD) simulations are used to obtain the dynamic input and output data sets of the 64-element Canadian supercritical water-cooled reactor (SCWR) in this study. Subsequently, the linear dynamic models of the reactor are obtained by the system identification technique and validated by the comparison with the results from CFD simulations. Based on the linear dynamic models, a feedback control system consists of three PI/PID controllers is constructed. The objective is to regulate the system back to the design point when the reactor is subjected to disturbances. Therefore, the performance of the designed feedback control system is also evaluated in this work. It shows that the designed control system can timely minimize the deviations and return the reactor back to the desired operating condition.

1. Introduction

Supercritical water-cooled reactors (SCWRs) are nuclear reactors that operate at pressures and temperatures above the critical point of water (22.1 MPa, 374°C). The SCWR is one of six Generation IV nuclear reactor concepts that is under development in several countries (Pioro, 2016). The concept of the SCWR is proposed based on the mature technologies of existing supercritical fossil-fueled power plants (SCFPP) and light water-cooled reactors (LWRs). Thus, the reactor coolant system in the SCWR is similar to that in the SCFPP, which is a once-through direct cycle. The main advantages of SCWRs are the potential of improved thermal efficiency and relatively simple plant system with fewer major components. The Canadian SCWR is a supercritical light water-cooled pressure-tube type nuclear reactor. The fuel channel of the reactor is vertically placed.

Since the thermophysical properties of the supercritical water vary significantly near the pseudocritical region, the understanding of dynamic characteristics of SCWRs is essential for the design and analysis of the control system. A few studies on the control system design for supercritical water-cooled type reactors have been conducted (Nakatsuka et al., 1998; ISHIWATARI et al., 2003; Sun et al., 2011; Sun and Jiang, 2012; Sun et al., 2014; Sun et al., 2015; Sun and Zhang, 2017; Maitri et al., 2017; Han et al., 2021). The earliest study of the control on the

SCWR was conducted by Nakatsuka et al. (1998) for the supercritical water-cooled fast reactor (SCFR) and then similar design method was applied in the further study (ISHIWATARI et al., 2003) for the supercritical high temperature thermal reactor. The stepwise responses of the reactor systems were analyzed with added perturbations. Based on the analysis, the relationship of inputs and outputs of the reactor system was obtained and the control system was established accordingly. The results showed that the reactor with the control system can operate stably when disturbances were added. Sun (Sun et al., 2011, 2014; Sun and Jiang, 2012) linearized the dynamic process in the reactor system and proposed a simplified one-dimensional dynamic model for the CANDU SCWR system. The dynamic characteristics of the control system were analyzed and the control relationship were the same as in (Nakatsuka et al., 1998; ISHIWATARI et al., 2003). Based on these studies, Sun (Sun et al., 2015; Sun and Zhang, 2017) also used different control methods, such as feedback controller, feed-forward controller (Sun et al., 2015) and linear parameter-varying controller (Sun and Zhang, 2017) to further improve the performance of the control system. In order to construct a feedback control system, a linear dynamic model is needed. The physical process is normally nonlinear. Therefore, several approaches can be used to linearize the process depending on the property of the process. If there is analytical solution for describing the physical process, the Taylor series expansion can be used and then only the linear terms are used. If experimental data are available, a linear dynamic

* Corresponding author.

E-mail addresses: hhan55@uwo.ca (H. Han), cchang@eng.uwo.ca (C. Zhang).

Nomenclature		<i>P</i>	Pressure, Pa
<i>g</i>	Gravitational acceleration, m/s ²	<i>Pr</i>	Prandtl number
<i>G</i>	Mass flux, kg/m ² ·s	<i>q</i>	Heat flux, W/m ²
<i>G_{r11}</i>	Transfer function representing the ratio of the outlet mass flow rate to the inlet mass flow rate in the Laplace transform domain	<i>s</i>	Complex variable in Laplace transform
<i>G_{r12}</i>	Transfer function representing the ratio of the outlet mass flow rate and the inlet temperature in the Laplace transform domain	<i>t</i>	Time, s
<i>G_{r13}</i>	Transfer function representing the ratio of the outlet mass flow rate to the heat flux in the Laplace transform domain	<i>T</i>	Temperature, °C
<i>G_{r21}</i>	Transfer function representing the ratio of the outlet temperature to the inlet mass flow rate in the Laplace transform domain	<i>U</i>	Input variables
<i>G_{r22}</i>	Transfer function representing the ratio of the outlet temperature to the inlet temperature in the Laplace transform domain	<i>u</i>	Velocity, m/s
<i>G_{r23}</i>	Transfer function representing the ratio of the outlet temperature to the heat flux in the Laplace transform domain	<i>Y</i>	Output variables
<i>G_{r31}</i>	Transfer function representing the ratio of the maximum wall temperature to the inlet mass flow rate in Laplace transform domain	<i>Greek Letters</i>	
<i>G_{r32}</i>	Transfer function representing the ratio of the maximum wall temperature to the inlet temperature in the Laplace transform domain	μ	Dynamic viscosity, Pa · s
<i>G_{r33}</i>	Transfer function representing the ratio of the maximum wall temperature to the heat flux in the Laplace transform domain	ρ	Density of a fluid, kg/m ³
<i>K_D</i>	Derivative gain	<i>Subscripts</i>	
<i>K_I</i>	Integral gain	<i>cr</i>	Critical
<i>K_P</i>	Proportional gain	<i>in</i>	Inlet
		<i>out</i>	Outlet
		<i>r</i>	Reactor
		<i>t</i>	Turbulent
		<i>w</i>	Wall
		max	Maximum
		<i>Acronyms</i>	
		CANDU	Canada Deuterium Uranium
		CFD	Computational Fluid Dynamics
		LWR	Light Water-Cooled Reactor
		SCFPP	Supercritical Fossil-Fueled Power Plant
		SCFR	Supercritical Water-Cooled Fast Reactor
		SCWR	Supercritical Water-Cooled Reactor
		SISO	Single-Input-Single-Output
		RGA	Relative Gain Array
		RSM	Reynolds Stress Model

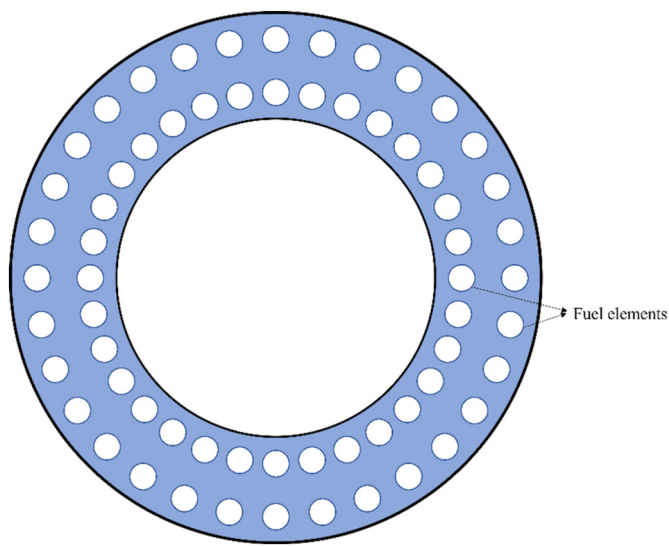


Fig. 1. Configuration of the 64-element fuel bundle.

model of the process can be obtained by system identification techniques depending on dynamic behaviors of inputs and outputs through introducing small perturbations at the design point. However, when the above two methods are not feasible, full scale computational fluid dynamics (CFD) simulations could be used instead to describe the physical

Table 1
Specifications of the 64-element Canadian SCWR.

Thermal power	2540 MW
Flow rate	1320 kg/s
Number of channels	336
Inlet temperature	350°C
Cladding temperature limit	850°C
Operating pressure	25 MPa
Heated length	5 m

process. Maitri et al. (2017) derived the dynamic relationships of inputs and outputs of the reactor by using the numerical results from CFD simulations of supercritical water flow in the heated tube. Perturbations were introduced and linear dynamic models were constructed and validated. Although the flow of the supercritical water in the reactor was simplified as a two-dimensional tube flow, this work proved that CFD simulations could be used as the method to obtain dynamic relationships between inputs and outputs of the supercritical water flow in the

Table 2
Disturbances added for time independent tests.

Time (s)	0	10	20	30	40	50	60
Inputs							
<i>m_{in}</i>	1	1	+10%	+10%	+10%	1	1
<i>T_{in}</i>	+10%	+10%	+10%	1	1	1	1
<i>q</i>	1	-10%	-10%	-10%	1	1	1

1 means the design point.

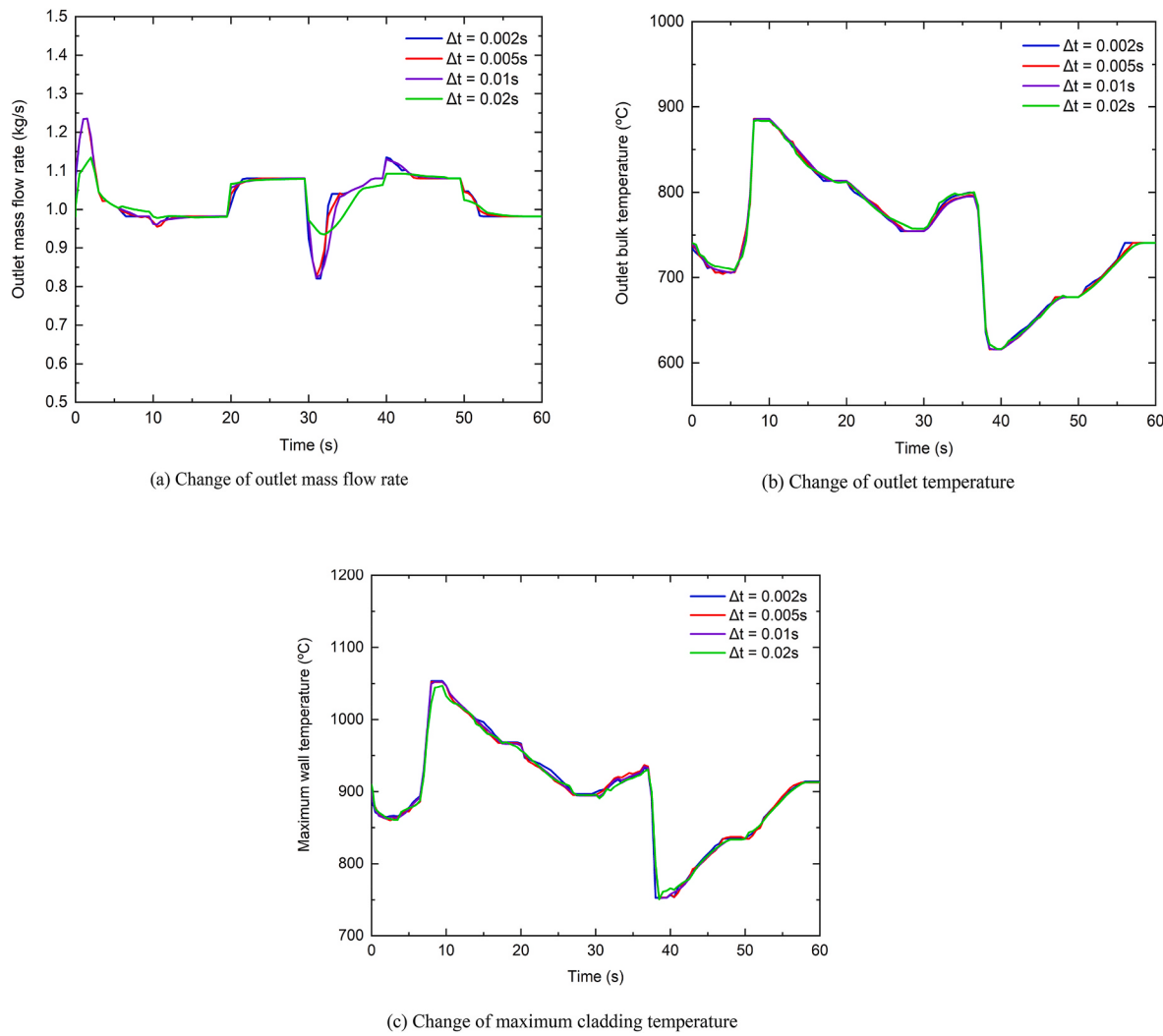


Fig. 2. Outputs with perturbations added using different time step sizes.

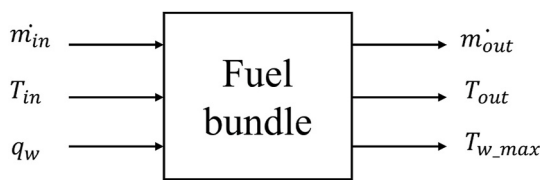


Fig. 3. Block representation of the dynamic model of the fuel bundle.

reactor. Studies used the similar methodology could be found in (Jiang et al., 2007; Meng et al., 2009; Zhang et al., 2011) for other transient physical processes. Han (Han et al., 2021) used the full scale three-dimensional CFD simulations of the supercritical water flow in the rod channels instead of the flow in a single tube and implemented a feedback control system. The performance of the control system has been evaluated around the operating point. In order to ensure the safety of a nuclear reactor, the maximum cladding surface temperature is an important parameter. The heat transfer characteristics of the supercritical water in the rod bundle directly influence the cladding temperature. Although the 64-element Canadian SCWR concept was proposed, there is still lack of studies in the design of the control system.

Therefore, in this study, we first obtain the dynamic relationships of inputs and outputs of the heat transfer process in the rod bundle and construct the linear dynamic models accordingly. This is followed by the

design of the feedback control system design for the simplified thermal hydraulic models of the 64-element reactor and the performance evaluation of the control system.

2. Reactor and its mathematical models

2.1. Configurations of 64-element fuel bundle of the Canadian SCWR

The fuel bundle used in the study is the newest proposed vertically oriented 64-element two-ring rod bundle (Yetisir et al., 2018) and the cross-section view of the fuel bundle is shown in Fig. 1. The fuel rods are symmetrically distributed with 32 rods in each ring. The heated length is 5 m. Operating parameters of the 64-element Canadian SCWR are summarized in Table 1 (Yetisir et al., 2018; Domínguez et al., 2016). The main heat transfer process in the reactor mainly occurs in the fuel bundle, which directly influences the safety of the reactor since the temperature in the reactor depends on the heat transfer process. Three controllable inputs of the reactor are the inlet mass flow rate of water, inlet temperature of water, and the heat flux on the fuel rod. The controlled outputs are the outlet mass flow rate, outlet temperature, and the maximum cladding temperature. Before constructing the control system, the relationship between inputs and outputs need to be determined, which is obtained with the help of transient CFD simulations of the fluid flow and heat transfer of the supercritical water in the fuel bundle.

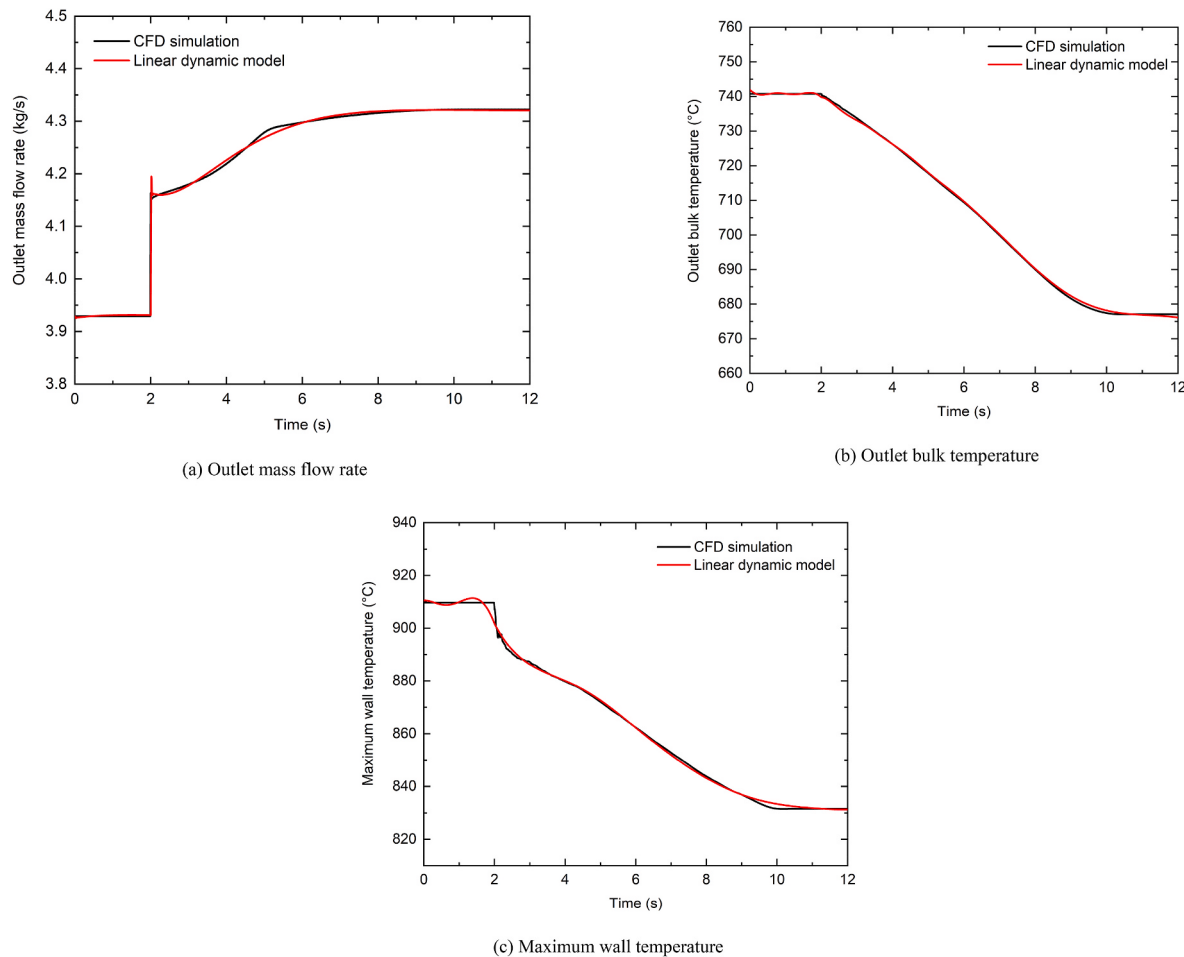


Fig. 4. Comparison of responses obtained by CFD simulations and linear dynamic model with a perturbation in the inlet mass flow rate.

2.2. Mathematical models used in CFD simulations

2.2.1. Governing equation

The fluid flow and heat transfer process in the fuel bundle is governed by the conservation equations of mass, momentum, and energy. The Reynolds averaged form of these equations are given as follows (ANSYS, 2013):

$$\frac{\partial \rho}{\partial t} + \frac{\partial \rho \bar{u}_i}{\partial x_i} = 0 \quad (1)$$

$$\frac{\partial \rho \bar{u}_i}{\partial t} + \frac{\partial (\rho \bar{u}_i \bar{u}_j)}{\partial x_j} = - \frac{\partial \bar{p}}{\partial x_i} + \frac{\partial}{\partial x_i} \left(\mu \frac{\partial \bar{u}_i}{\partial x_j} - \rho \bar{u}_i \bar{u}'_j \right) + \rho g_i \quad (2)$$

$$\frac{\partial (\rho c_p T)}{\partial t} + \frac{\partial}{\partial x_i} (\bar{u}_i \rho c_p T) = \frac{\partial}{\partial x_i} \left[\left(\lambda + \frac{c_p \mu_t}{Pr_t} \right) \frac{\partial T}{\partial x_i} \right] \quad (3)$$

2.2.2. Turbulent models

In order to solve the Reynolds stress term ($\rho \bar{u}_i \bar{u}'_j$), which needs an appropriate treatment of the turbulent Prandtl number (Pr_t) for the heat transfer of the supercritical water in the fuel bundle, the previously validated Reynolds stress model (RSM) with a variable Pr_t model is used for the turbulent modeling in this study. The transport equation for the RSM is given as (ANSYS, 2013):

$$\frac{\partial}{\partial t} \left(\rho \bar{u}_i \bar{u}'_j \right) + \frac{\partial}{\partial x_k} \left(\rho u_k \bar{u}_i \bar{u}'_j \right) = - \frac{\partial}{\partial x_k} \left[\rho \bar{u}_i \bar{u}'_j \bar{u}_k + p' (\delta_{kj} \bar{u}_i + \delta_{ik} \bar{u}'_j) \right]$$

Local time derivative $C_{ij} \equiv \text{Convection}$ $D_{T,ij} \equiv \text{Turbulent Diffusion}$

$$\begin{aligned}
 & + \frac{\partial}{\partial x_k} \left[\mu \frac{\partial}{\partial x_k} (\bar{u}_i \bar{u}'_j) \right] - \rho \left(\bar{u}_i \bar{u}'_k \frac{\partial \bar{u}_j}{\partial x_k} + \bar{u}'_j \bar{u}_k \frac{\partial \bar{u}_i}{\partial x_k} \right) \\
 & D_{L,ij} \equiv \text{Molecular Diffusion} \quad P_{ij} \equiv \text{Stress Production} \\
 & - \rho \beta \left(g_i \bar{u}_j \theta + g_j \bar{u}_i \theta \right) + \overbrace{p' \left(\frac{\partial \bar{u}_i}{\partial x_j} + \frac{\partial \bar{u}'_j}{\partial x_i} \right)}^{G_{ij} \equiv \text{Buoyancy Production} \quad \varphi_{ij} \equiv \text{Pressure Strain}} \\
 & - 2 \mu \overbrace{\frac{\partial \bar{u}_i}{\partial x_k} \frac{\partial \bar{u}'_j}{\partial x_k}}^{\varepsilon_{ij} \equiv \text{Dissipation}} - 2 \rho \Omega_k \left(\bar{u}_j \bar{u}'_m \varepsilon_{ikm} + \bar{u}'_j \bar{u}_m \varepsilon_{jkm} \right) \\
 & F_{ij} \equiv \text{Production by System Rotation} \\
 & + \underbrace{S_{user}}_{\text{User-Defined Source Term}}
 \end{aligned} \quad (4)$$

The variable Pr_t model used in this work (Han and Zhang, 2022) is:

$$Pr_t = \begin{cases} 0.4 \frac{\mu_t}{\mu} < 0.2 \\ 0.3 + 0.03 \times (P/P_{cr}) \times Pr \times (\mu_t/\mu) \times (q/G) & 0.2 \leq \mu_t/\mu \leq 10 \\ 0.85 & \mu_t/\mu > 10 \end{cases} \quad (5)$$

The transient CFD simulations of the supercritical water flow in the fuel bundle were conducted by ANSYS FLUENT to capture the dynamic characteristics of inputs and outputs. The control volume method is used to discretize the physical domain and convert the partial differential equations to sets of algebraic equations. Accordingly, algebraic equations are solved iteratively until the convergence criteria are satisfied.

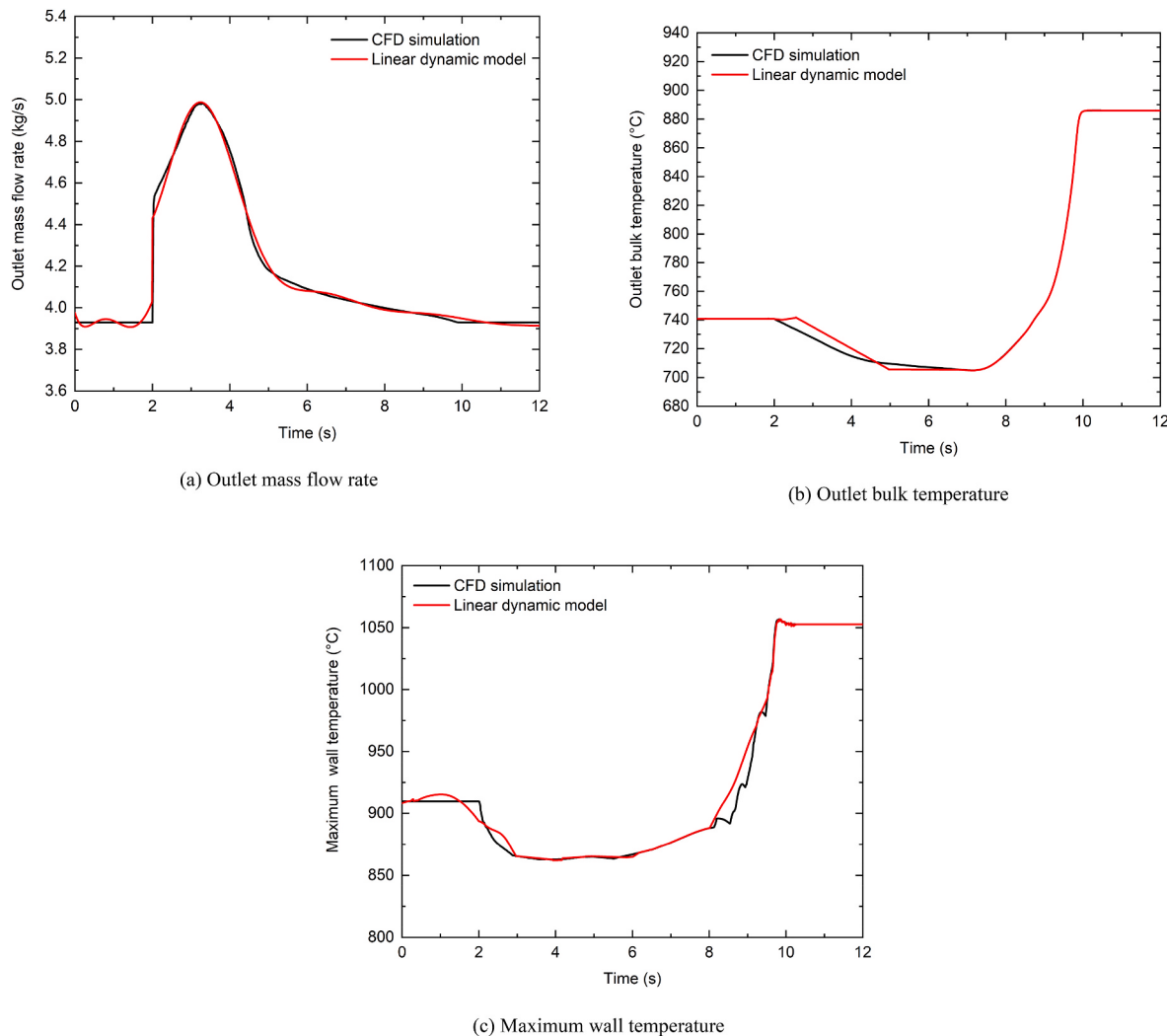


Fig. 5. Comparison of responses obtained by CFD simulations and linear dynamic model with a perturbation in the inlet temperature.

3. Construction of the linear dynamic models

3.1. Time independent tests

The dynamic relationship between inputs and outputs are obtained by transient CFD simulations, which is the basis of the construction of dynamic models. Therefore, it is important to determine an appropriate time step size used in transient simulations so that the results from transient simulations are independent of the time step size. In the time independent tests, continuous perturbations of inputs are added at each 10 s and lasts for 20 s starting from the design point (0 s). Table 2 shows the order of added perturbations in 60 s. The respective variations of all outputs captured by transient CFD simulations with various time step sizes are plotted in Fig. 2. It is seen that there are small differences between the simulation results when the time step is less than 0.01 s. Therefore, the time step size 0.01 s is used in transient CFD simulations to obtain the dynamic relationship between inputs and outputs.

3.2. Construction of transfer functions

The dynamic model for the fuel bundle consists of three inputs and three outputs, as illustrated in Fig. 3. The governing equations for the fluid flow and heat transfer of the supercritical water are highly nonlinear. It is unrealistic to directly linearize governing equations. Therefore, a linear dynamic model of the fuel bundle is constructed on

the basis of dynamic relationship between inputs and outputs obtained from transient CFD simulations.

The methodology to obtain the linear dynamic model of the fuel bundle is described as follows. 10% step perturbation of only one input is added to the steady state at $t = 2$ s and the resulting changes of all three outputs are obtained through transient CFD simulations. This process is repeated for each input variable. Since there are three input variables, the recorded responses would consist of 9 sets of input and output variables. The flow and heat transfer process in the fuel bundle can be expressed in matrix form of transfer functions:

$$Y_{r(s)} = \begin{bmatrix} Y_{r1(s)} \\ Y_{r2(s)} \\ Y_{r3(s)} \end{bmatrix} = G_{r(s)} U_{r(s)} = \begin{bmatrix} G_{r11}(s) & G_{r12}(s) & G_{r13}(s) \\ G_{r21}(s) & G_{r22}(s) & G_{r23}(s) \\ G_{r31}(s) & G_{r32}(s) & G_{r33}(s) \end{bmatrix} \begin{bmatrix} U_{r1(s)} \\ U_{r2(s)} \\ U_{r3(s)} \end{bmatrix} \quad (6)$$

From these data sets, the least square method-based system identification technique is used to choose the best fitting for the dynamic models (Ljung). Since the transfer function is defined as the ratio of the Laplace transform of the output to the Laplace transform of the input by assuming initial conditions are zero, the construction of transfer functions for linear dynamic models is based on changes of respective inputs and outputs relative to their values at the design point due to the introduction of disturbances. The parameters of the dynamic models are regulated to minimize the sum of the squares of differences between results from CFD simulations and the outputs from the dynamic models. Transfer functions of the linear dynamic models in the Laplace form are

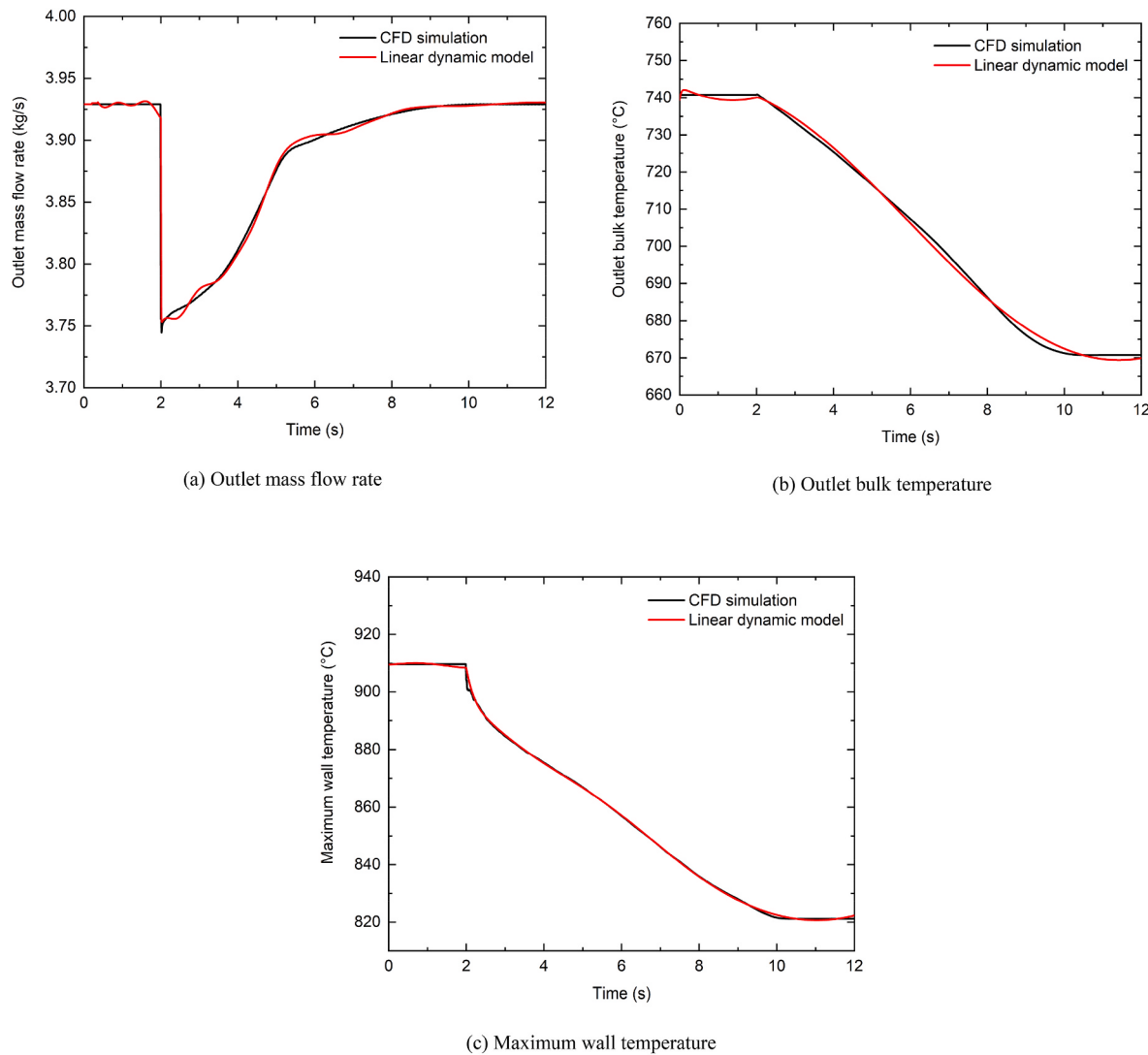


Fig. 6. Comparison of responses obtained by CFD simulations and linear dynamic model with a perturbation in the heat flux introduced.

Table 5
Specifications of controllers.

Controllers	K_P	K_I	K_D	Rising time (s)	Settling time (s)	Overshoot (%)
PI_1	0.7413	116.8418		0.0265	0.0763	5.16
PI_2	0.045	0.0902		9.06	6.23	10.2
PID_3	6.0910e+3	5.4748e+4	67.63598	0.221	2.26	14.2

shown as follows:

$$G_{r11(s)} = \frac{42.95s^2 + 52.54s + 44.28}{s^3 + 68.48s^2 + 96.16s + 44.29} \quad (7)$$

$$G_{r12(s)} = \frac{0.01139s^5 + 0.02959s^4 + 0.1029s^3 + 0.1088s^2 + 0.1427s + 0.03218}{s^5 + 2.707s^4 + 8.535s^3 + 10.62s^2 + 10.94s + 3.182} \quad (8)$$

$$G_{r13}(s) = \frac{0.0004862s^8 + 0.002397s^7 + 0.03164s^6 + 0.1042s^5 + 0.5411s^4 + 1.088s^3 + 2.705s^2 + 2.906s + 1.057}{s^9 + 262.7s^8 + 1501s^7 + 1.655 \times 10^4 s^6 + 5.982 \times 10^4 s^5 + 2.491 \times 10^5 s^4 + 4.864 \times 10^5 s^3 + 8.496 \times 10^5 s^2 + 7.166 \times 10^5 s + 2.13 \times 10^5} \quad (9)$$

$$G_{r21}(s) = \frac{-35.43s^6 - 50.78s^5 - 797.6s^4 - 170s^3 - 1537s^2 + 5183s + 3600}{s^7 + 4.627s^6 + 30.51s^5 + 92.96s^4 + 175.4s^3 + 202.8s^2 + 53.42s + 22.47} \quad (10)$$

$$G_{r22}(s) = \frac{166.2s^{15} + 6078s^{14} + 1.071 \times 10^4 s^{13} + 3.949 \times 10^5 s^{12} + 1.82 \times 10^5 s^{11} + 7.999 \times 10^5 s^{10} + 9.215 \times 10^5 s^9 + 6.96 \times 10^7 s^8 - 1.624 \times 10^6 s^7 + 2.763 \times 10^8 s^6 - 2.191 \times 10^7 s^5 + 4.669 \times 10^8 s^4 - 4.11 \times 10^7 s^3 + 2.655 \times 10^8 s^2 - 1.392 \times 10^7 s + 2.132 \times 10^7}{s^{19} + 13.11s^{18} + 179.1s^{17} + 1429s^{16} + 1.043 \times 10^4 s^{15} + 5.761 \times 10^4 s^{14} + 2.716 \times 10^5 s^{13} + 1.101 \times 10^6 s^{12} + 3.575 \times 10^6 s^{11} + 1.11 \times 10^7 s^{10} + 2.46 \times 10^7 s^9 + 6.09 \times 10^7 s^8 + 8.591 \times 10^7 s^7 + 1.767 \times 10^8 s^6 + 1.376 \times 10^8 s^5 + 2.429 \times 10^8 s^4 + 7.938 \times 10^7 s^3 + 1.215 \times 10^8 s^2 + 6.714 \times 10^6 s + 9.625 \times 10^6} \quad (11)$$

$$G_{r23}(s) = \frac{10^{-4}(2.576s^3 + 6.862s^2 + 4.012s + 2.553)}{s^4 + 2.373s^3 + 2.146s^2 + 1.093s + 0.299} \quad (12)$$

$$G_{r31}(s) = \frac{20.46s^4 + 281.9s^3 + 448.8s^2 + 909.5s + 211.8}{s^5 + 1.76s^4 + 5.969s^3 + 6.427s^2 + 4.194s + 1.101} \quad (13)$$

4. Design of the feedback control system

The objective of the feedback control system is to regulate outputs back to the design point in time when the fuel bundle is subjected to perturbations. As shown above, the fuel bundle has multiple inputs and outputs. When the perturbation is added to one input, all outputs will change. Therefore, the interaction degree of inputs and outputs at the

$$G_{r32}(s) = \frac{-3.388s^8 - 10.24s^7 - 162.5s^6 - 404.6s^5 - 1601s^4 - 2369s^3 - 977s^2 - 640.5s + 53.52}{s^9 + 1.862s^8 + 55.11s^7 + 80.76s^6 + 674s^5 + 588.6s^4 + 1118s^3 + 670.3s^2 + 389.8s + 9.111} \quad (14)$$

$$G_{r33}(s) = \frac{10^{-4}(73.78s + 7.294)}{s^6 + 4.655s^5 + 15.79s^4 + 20.64s^3 + 14.44s^2 + 7.749s + 0.7372} \quad (15)$$

3.3. Validation of transfer functions

The above transfer functions derived from CFD simulations need to be evaluated whether they can characterize the dynamic behaviors of the nonlinear system around the design points. The dynamic responses generated by the linear dynamic model and results from transient CFD simulations are compared when inputs are subjected to step perturbations. Figs. 4–6 exhibit the comparisons at the conditions of step perturbations of inlet mass flow rate, inlet temperature, and heat flux, respectively.

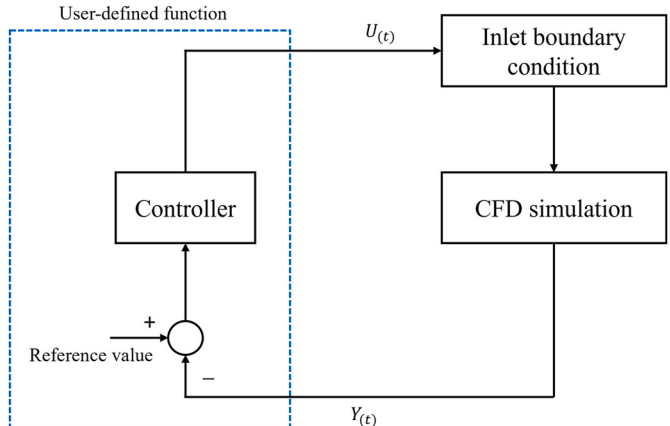


Fig. 8. Flowchart of embedding controllers in the CFD simulations.

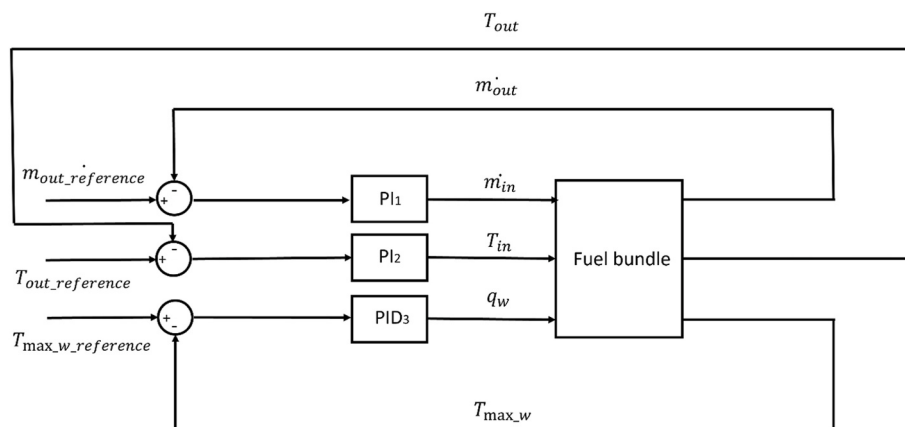


Fig. 7. Block representation of the feedback control system.

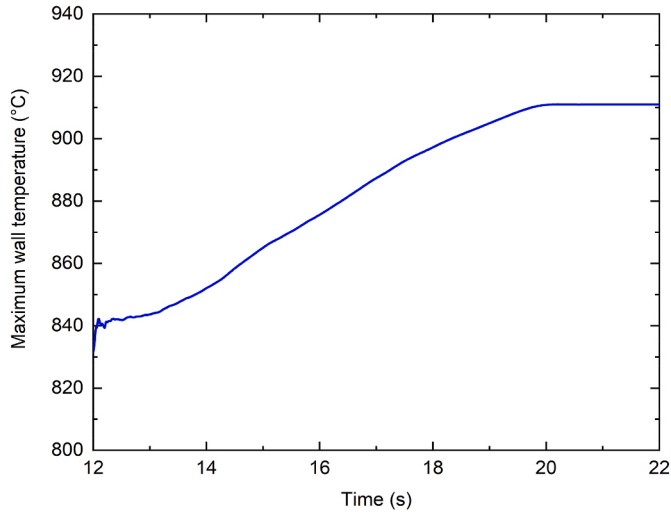
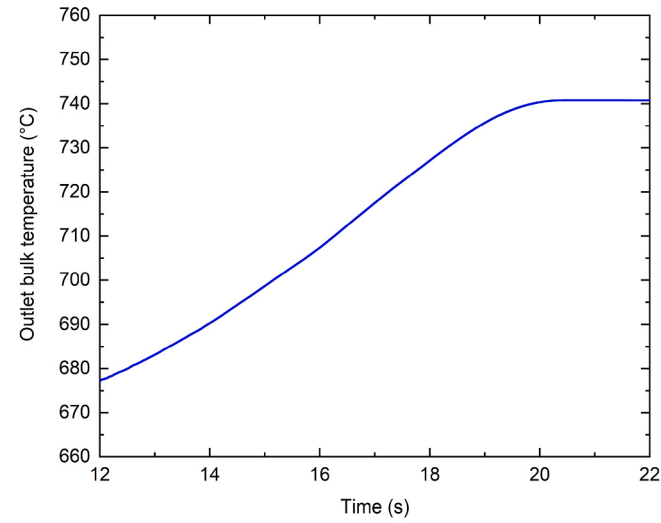
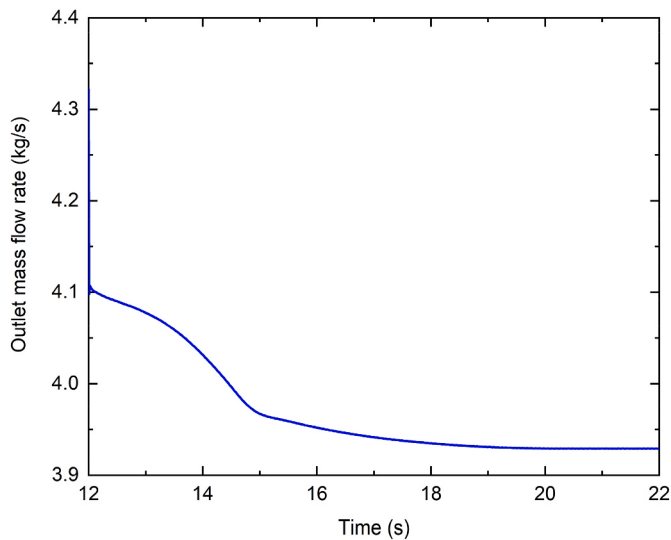


Fig. 9. Output responses by CFD simulations when the system is subjected to the perturbation in the inlet mass flow rate.

steady state is investigated in this study, so that the most relevant input and output can be identified. The relative gain array (RGA) is commonly used to evaluate the cross-coupling between inputs and outputs of a system at the steady state condition (Bristol, 1966; Skogestad and

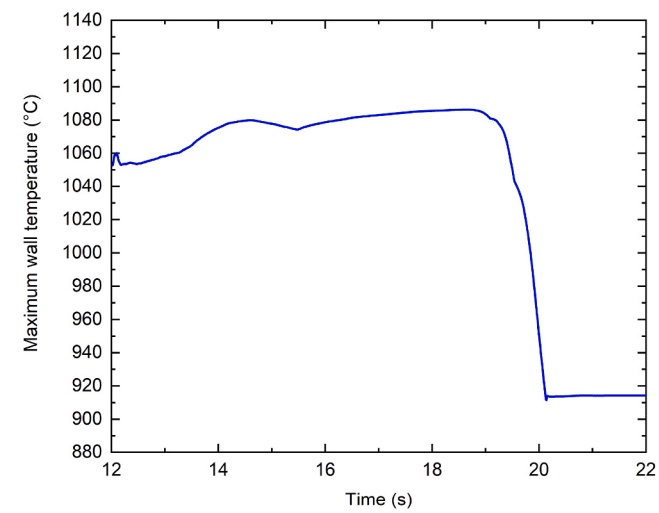
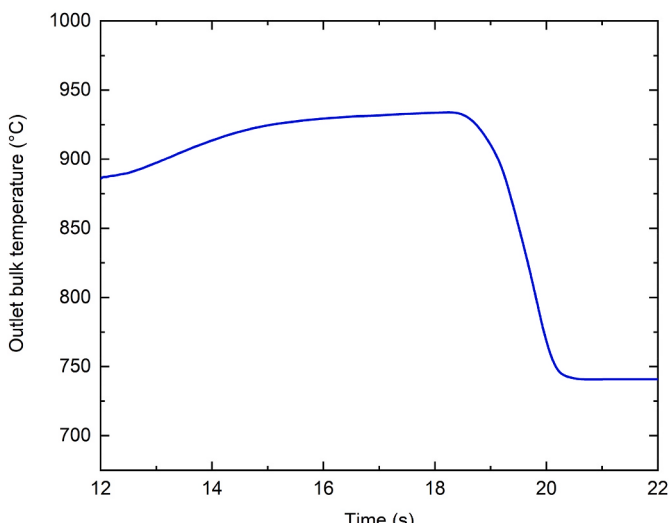
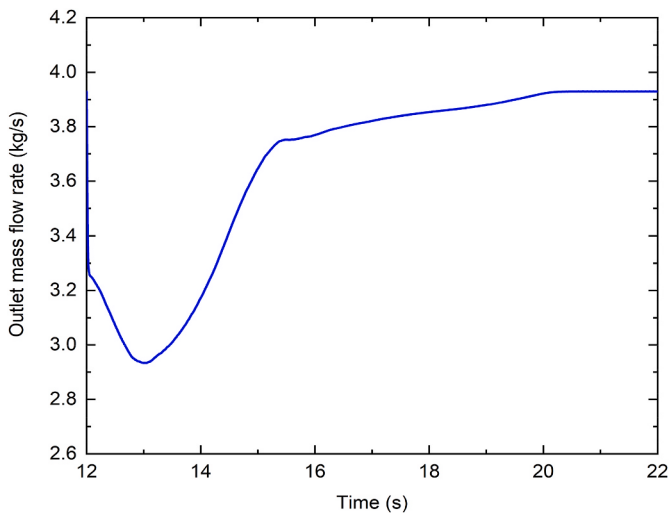


Fig. 10. Output responses by CFD simulations when the system is subjected to the perturbation in the inlet temperature.

Postlethwaite, 2005). The RGA is the normalized form of the gain matrix of a system, which describes the influence of an input on an output with respect to that on the rest outputs. The gain matrix K_r of the fuel bundle is obtained from $G_{r(s)}$ as:

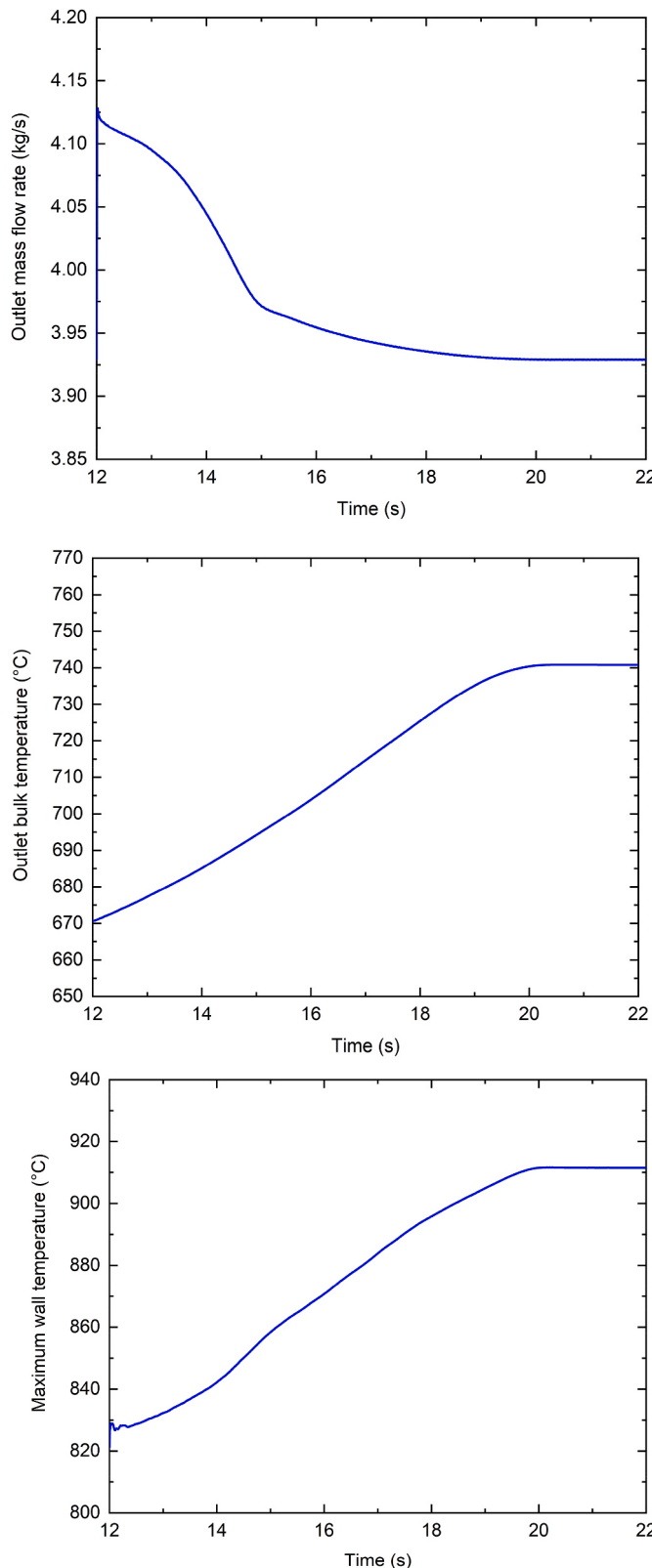


Fig. 11. Output responses by CFD simulations when the system is subjected to the perturbation in the heat flux on the fuel rod.

$$K_r = \begin{bmatrix} 0.9996 & 0.01 & 4.96 \times 10^{-6} \\ 160.23 & 2.22 & 8.54 \times 10^{-4} \\ 192.29 & 5.87 & 9.89 \times 10^{-4} \end{bmatrix} \quad (16)$$

Accordingly, the RGA of the system at the design point can be obtained as follows:

$$RGA_r = \begin{bmatrix} 1.37 & 0.00 & -0.37 \\ 0.00 & 0.98 & 0.02 \\ -0.37 & 0.02 & 1.35 \end{bmatrix} \quad (17)$$

Normally the relative gains of the respective input and output near 1 should be paired and negative relative gains should not be paired. Therefore, the fuel bundle can be seen as a diagonally dominant system at the design point. The interaction between the respective input and output can be determined as: the outlet mass flow rate mainly depends on the inlet mass flow rate, the outlet temperature is determined primarily by the inlet temperature, and the maximum cladding temperature is affected most by the heat flux on the fuel rod. Consequently, the fuel bundle can be regarded as a multiple single-input-single-output (SISO) system. In the feedback control system, one PID controller is used for each most relevant input and output pair to regulate the corresponding output back to the design point. Therefore, three controllers are needed for this three-input and three-output system. To satisfy the purpose of regulating deviations to zero when the system is subjected to perturbations, PI/PID type controllers are selected. The general transfer function from a PID controller could be expressed as (Nise, 2008):

$$C_{(s)} = K_p + K_I/s + K_D s \quad (18)$$

where K_p , K_I , and K_D are the proportional, integral, and derivative gains. These gains are adjusted to satisfy the following design specifications: the overshoot is less than 15%, the rise time and settling time are both below 10 s. Table 5 shows these gains for the three controllers.

5. Evaluation of the performance of the feedback control system

The block diagram of the feedback control system for the fuel bundle is presented in Fig. 7. Since the control system is constructed according to linear dynamic models, it is essential to evaluate the performance of the feedback control system at nonlinear conditions.

The performance evaluation is carried out through incorporating the feedback control system into the nonlinear transient CFD simulations. Controllers in the system are activated after the perturbation of the input has been held for 12 s. Then, the PID controllers are activated to regulate the system. This is carried out through embedding the designed control system into the transient CFD simulations through user-defined functions, which is given in the flowchart shown in Fig. 8. The deviations of the output results of the transient CFD simulations from the design point values at each time step are taken as the input variables for the controllers and the outputs of the controllers are the inputs for the CFD simulations in the following time step. Therefore, the controllers and the transient CFD simulations form a closed loop. The time step size for transient CFD simulations and the sampling time interval of the control system are both 0.01 s. Figs. 9–11 show the responses of outputs from nonlinear CFD simulations when the system is subjected to the perturbation of the three inputs, respectively. It can be seen that the feedback control system can regulate outputs to design point in time at around 8 s.

6. Conclusion

The knowledge of the dynamic behaviors of the fluid flow and heat transfer in the reactor is essential for safe operation. In this study, the feedback control system for the reactor is developed. The dynamic relationship between inputs and outputs of the reactor were obtained from transient CFD simulations, and then the results from the linear dynamic models are validated through the comparison of the results from nonlinear transient CFD simulations. Based on the linear dynamic models, three PID controllers are synthesized in the feedback control system to regulate the inputs for the SCWR so that the deviation of the SCWR outputs from the designed values could be minimized

accordingly. In addition, the performance of the feedback control system was evaluated. The results showed that the control system can regulate the reactor to the design point in time when it is subjected to disturbances.

Declaration of competing interest

The authors declare that they have no known competing financial interests or personal relationships that could have appeared to influence the work reported in this paper.

Data availability

Data will be made available on request.

Acknowledgements

This work was supported by the Natural Sciences and Engineering Research Council of Canada (NSERC) Discovery grant.

References

- ANSYS, 2013. Ansys Fluent Theory Guide.**
- Bristol, E., 1966. On a new measure of interaction for multivariable process control. *IEEE Trans. Automat. Control* 11 (1), 133–134. <https://doi.org/10.1109/TAC.1966.1098266>.
- Dominguez, A.N., Onder, N., Rao, Y., Leung, L., 2016. Evolution of the CANADIAN SCWR fuel-assembly concept and assessment of the 64 element assembly for THERMALHYDRAULIC performance. *CNL Nucl. Rev.* 1–18. <https://doi.org/10.12943/CNR.2015.00057>.
- Han, H., Zhang, C., 2022. A modified turbulent model for the supercritical water flows in the vertical upward channels. *J. Supercrit. Fluids* 187, 105632. <https://doi.org/10.1016/j.supflu.2022.105632>.
- Han, H., Zhang, C., Jiang, J., 2021. Dynamic models and control system design for heated channels in a Canadian SCWR. *Ann. Nucl. Energy* 151, 107973. <https://doi.org/10.1016/j.anucene.2020.107973>.
- Ishiwatari, Y., Oka, Y., Koshizuka, S., 2003. Control of a high temperature supercritical pressure light water cooled and moderated reactor with water rods. *J. Nucl. Sci. Technol.* 40 (5), 298–306. <https://doi.org/10.1080/18811248.2003.9715359>.
- Jiang, Q., Zhang, C., Jiang, J., 2007. A CFD assisted control system design with applications to NO_x control in a FGR furnace. *Combust. Theor. Model.* 11 (3), 469–481. <https://doi.org/10.1080/13647830601040019>.
- L. Ijung, "System Identification Toolbox: User's Guide, R2022a."
- Maitri, R.V., Zhang, C., Jiang, J., 2017. Computational fluid dynamic assisted control system design methodology using system identification technique for CANDU supercritical water cooled reactor (SCWR). *Appl. Therm. Eng.* 118, 17–22. <https://doi.org/10.1016/j.applthermaleng.2017.02.079>.
- Meng, Q., Wang, Y., Yan, X., Li, Z., 2009. CFD assisted modeling for control system design: a case study. *Simulat. Model. Pract. Theor.* 17 (4), 730–742. <https://doi.org/10.1016/j.simpat.2009.01.003>.
- Nakatsuka, T., Oka, Y., Koshizuka, S., 1998. Control of a fast reactor cooled by supercritical light water. *Nucl. Technol.* 121 (1), 81–92. <https://doi.org/10.13182/NT98-A2821>.
- Nise, N.S., 2008. *Control Systems Engineering*, fifth ed. Wiley, Hoboken, NJ.
- Pioro, I.L. (Ed.), 2016. *Handbook of Generation IV Nuclear Reactors*, first ed. Elsevier—Woodhead Publishing, Duxford, UK. <https://doi.org/10.1016/C2014-0-01699-1>.
- Skogestad, S., Postlethwaite, I., 2005. *Multivariable Feedback Control : Analysis and Design*, second ed. John Wiley, Chichester, England.
- Sun, P., Jiang, J., 2012. Construction and analysis of a dynamic model for a Canadian direct-cycle SCWR for control system studies. *Nucl. Technol.* 180 (3), 399–421. <https://doi.org/10.13182/NT12-A15352>.
- Sun, P., Zhang, J., 2017. Control strategy study for once-through direct cycle Canadian SCWRs. *Prog. Nucl. Energy* 98, 202–212. <https://doi.org/10.1016/j.pnucene.2017.03.024>.
- Sun, P., Jiang, J., Shan, J., 2011. Construction of dynamic model of CANDU-SCWR using moving boundary method. *Nucl. Eng. Des.* 241 (5), 1701–1714. <https://doi.org/10.1016/j.nucengdes.2011.02.017>.
- Sun, P., Jiang, J., Wang, K., 2014. Decoupling control of Canadian supercritical water-cooled reactors. *Nucl. Technol.* 185 (3), 239–258. <https://doi.org/10.13182/NT12-130>.
- Sun, P., Wang, B., Zhang, J., Su, G., 2015. Control of Canadian once-through direct cycle supercritical water-cooled reactors. *Ann. Nucl. Energy* 81, 6–17. <https://doi.org/10.1016/j.anucene.2015.03.008>.
- Yetisir, M., Hamilton, H., Xu, R., Gaudet, M., Rhodes, D., King, M., Andrew, K., Benson, B., 2018. Fuel assembly concept of the Canadian supercritical water-cooled reactor. *J. Nucl. Eng. Radiat. Sci.* 4 (1), 1–7. <https://doi.org/10.1115/1.4037818>.
- Zhang, R., Zhang, C., Jiang, J., 2011. A new approach to design a control system for a FGR furnace using the combination of the CFD and linear system identification techniques. *Combust. Theor. Model.* 15 (2), 183–204. <https://doi.org/10.1080/13647830.2010.532571>.